electronics

MDPI

Article

Ultra-Wideband Pentagonal Fractal Antenna with Stable Radiation Characteristics for Microwave Imaging Applications

Muhammad Abbas Khan [1], Umair Rafique [2,*], Hüseyin Şerif Savci [3], Anis Nurashikin Nordin [4], Saad Hassan Kiani [5,6] and Syed Muzahir Abbas [7,*]

1 Department of Electrical Engineering, Balochistan University of Information Technology, Engineering and Management Sciences, Quetta 87300, Pakistan; muhammad.abbas@buitms.edu.pk
2 Department of Information Engineering, Electronics, and Telecommunications, Sapienza University of Rome, 00184 Rome, Italy
3 Electrical and Electronics Engineering Department, Istanbul Medipol University, Istanbul 34810, Turkey; hsavci@medipol.edu.tr
4 Department of Electrical & Computer Engineering, International Islamic University Malaysia, Kuala Lumpur 43200, Malaysia; anisnn@iium.edu.my
5 Department of Electrical Engineering, IIC University of Technology, Phnom Penh 121206, Cambodia; iam.kiani91@gmail.com
6 Smart Systems Engineering Laboratory, College of Engineering, Prince Sultan University, Riyadh 11586, Saudi Arabia
7 Faculty of Science and Engineering, School of Engineering, Macquarie University, Sydney, NSW 2109, Australia
* Correspondence: umair.rafique@uniroma1.it (U.R.); syed.abbas@mq.edu.au (S.M.A.)

Abstract: For microwave imaging applications, a design for an ultra-wideband (UWB) fractal antenna is presented. The antenna design is composed of a pentagonal fractal patch radiator fed by a modified co-planar waveguide (CPW) ground plane. It is built on a low-loss Rogers RT/Duroid 5880 dielectric substrate with a dimensions of 24 × 30 × 0.787 mm^3. According to the measurements, the designed antenna offers a fractional bandwidth of 123.56% ranging from 3 GHz to 12.7 GHz. In addition, a maximum gain of 3.6 dBi is achieved at 8.5 GHz. From the results, it is also observed that the proposed antenna structure attains constant radiation characteristics in the operating bandwidth, which is useful for microwave imaging applications. The time domain analysis of the proposed design is also performed, and it is observed that the designed antenna offers a group delay of ≤1.5 ns, which ensures minimum pulse distortion.

Keywords: microwave imaging; ultra-wideband; fractal antenna; co-planar waveguide; fractional bandwidth; group delay

Citation: Khan, M.A.; Rafique, U.; Savci, H.Ş.; Nordin, A.N.; Kiani, S.H.; Abbas, S.M. Ultra-Wideband Pentagonal Fractal Antenna with Stable Radiation Characteristics for Microwave Imaging Applications. *Electronics* **2022**, *11*, 2061. https://doi.org/10.3390/electronics11132061

Academic Editor: Andrea Randazzo

Received: 9 June 2022
Accepted: 29 June 2022
Published: 30 June 2022

1. Introduction

Near-field microwave imaging has gotten a lot of attention in recent years, especially for detecting and localizing cancer tissues in the human body [1]. Microwave imaging offers promising solutions for a number of biological applications [2] when compared to existing approaches such as ultrasound [3] and mammography [4]. In this technique, short pulses of low power are emitted by antennas towards the human body. The backscattered radiation is then collected by the antennas and processed to form an image. One of the examples is shown in Figure 1. From the figure, one can observe that multiple antennas operating in the near field are placed around the breast. The antennas forming the array are sequentially selected to transmit pulses into the breast. Then, the backscattered signals are collected by the receiving antennas. Finally, a suitable signal processing technique is applied to backscattered signals for image reconstruction.

Microwave imaging antennas should have a wide bandwidth and be able to provide constant radiation performance. Furthermore, the antenna's time domain performance

should be sufficient to allow transmitted pulses to pass through human tissues with minimal signal distortion. Ultra-wideband (UWB) technology may be useful in meeting these criteria as the pulse duration in UWB systems is often on the scale of a few nanoseconds, resulting in a bandwidth of a few gigahertz. In addition, the antenna size should be small enough so that it can easily be integrated into microwave imaging systems. To accommodate this requirement, researchers presented a variety of antenna designs. From the presented designs, planar antennas received a lot of attention due to their small size and light weight.

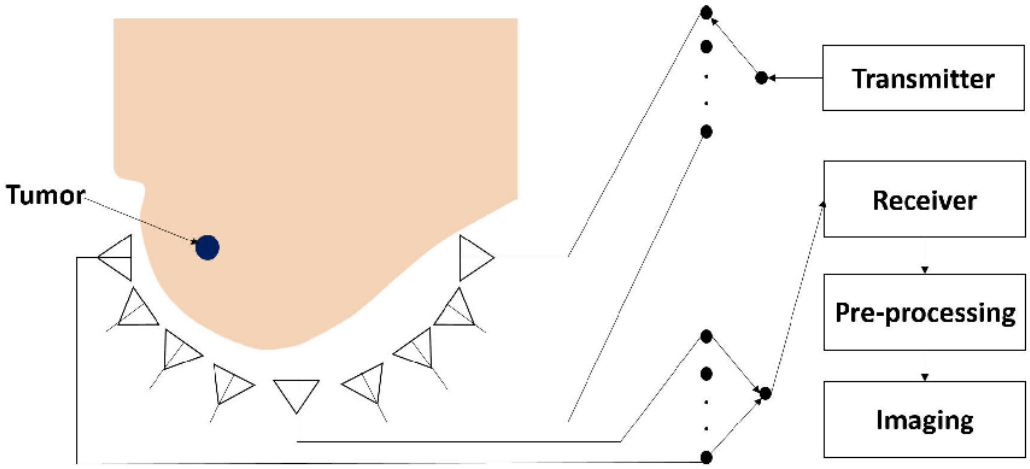

Figure 1. A typical near-field microwave imaging system for breast cancer detection [5] (Reprinted from an open access article published under Creative Commons Attribution 4.0 License).

For UWB microwave imaging systems, the authors in [6] presented a modified square monopole antenna design. In the ground plane, a pair of loop sleeves was designed, which tend to achieve an impedance bandwidth in the frequency range of 3.19–11.03 GHz. Although the designed antenna offers a wide impedance bandwidth, its efficiency is decreasing with an increase in frequency. For body-centric imaging applications, Danjuma et al. [7] designed a co-planar waveguide (CPW)-fed quasi-cross slot-based circular monopole antenna. The presented antenna can operate at frequencies ranging from 3 GHz to more than 11 GHz. A Hibiscus petal-like patch antenna was presented in [8] for microwave imaging systems. To obtain an impedance bandwidth in the frequency range of 3.04–11 GHz, a tapered microstrip feed line and a partial trapezoid ground plane were used. The performance of the antenna was evaluated in the time domain and a high value of group delay was observed for the side-by-side configuration, which is not useful for microwave imaging applications. In [9], an octagonal planar antenna was designed to detect malignant tissues in the human body. To achieve UWB response, the radiating element was fed by a 50 Ω microstrip feeding line and a step impedance transformer. For improved radiation characteristics, a circular slot including a symmetrical metal cross was designed in the octagonal radiator. From the presented configuration, the authors achieved an impedance bandwidth of 12 GHz from 3 GHz to 15 GHz.

Lee et al. [10] introduced a UWB-resistive dipole antenna for microwave imaging applications. They demonstrated that the designed dipole antenna offers minimal internal reflections compared to other UWB antenna structures. They employed chip resistors on both arms of the dipole antenna according to the technique presented in [11], and observed a UWB response ranging from 1 GHz to 10 GHz. However, this kind of configuration led to a large antenna size and was complex in nature. A square fractal monopole antenna with a slotted partial ground plane was presented in [12] for imaging purposes. The designed antenna-measured results demonstrate that it offers a fractional bandwidth (FBW) of 117.88% from 3.1 GHz to 12 GHz. A modified square monopole antenna design was presented in [13] for medical applications. With the use of modified square patch

and inverted U-shaped parasitic elements, the authors achieved a 5.2 GHz impedance bandwidth from 3.8 GHz to 9 GHz. Another square monopole antenna with a T-slot-loaded ground plane was designed in [14] for UWB microwave imaging applications. In addition to the T-slot, a parasitic element with a π shape was placed beneath the microstrip line to achieve a UWB response in the frequency range of 2.91–14.72 GHz.

Ojaroudi and Ghadimi [15] utilized the same technique as presented in [14] to design a multi-resonance UWB antenna for microwave imaging applications. In this design, an E-shaped slot was etched in the ground plane, and an E-shaped parasitic structure was designed behind the microstrip feeding line. The presented configuration extends the upper-frequency limit of the antenna from 10.3 GHz to 15 GHz. The designs presented in [14,15] were able to provide a UWB response, but their radiation characteristics were not stable over the operating bandwidth. In [16], three T-shaped slots were etched in the ground plane to achieve resonance ranging from 2.96 GHz to 15.8 GHz. Lasemi and Atlasbaf [17] designed compact UWB fractal antennas for breast tumor detection. The Sierpinski gasket configuration was used for one antenna, and a ring-inscribed hexagonal fractal antenna was used for the other. According to the measurements, the designed antennas operate well from 2.95 GHz to 12 GHz. However, the time domain performance of the presented designs reveals that the transmission phase of the antennas was not stable over the operating bandwidth, which ultimately led to pulse distortion.

A negative index mematerial-based planar antenna was designed in [18] for microwave imaging applications. To achieve a compact size, the edges of the triangular patch were loaded with four left-handed metamaterial unit cells. To achieve negative permittivity and permeability, each metamaterial unit cell was composed of a modified split-ring resonator (SRR) and a capacitance-loaded strip. Measurement results show that the presented antenna operates well from 3.4 GHz to 12.5 GHz and offers a maximum gain of 5.16 dBi at 10.15 GHz. The same technique was utilized in [19] to design a compact planar metamaterial antenna. In this design, a trapezoidal patch radiator was used, which was fed through a stepped tapered microstrip feed line. The presented antenna was able to operate in the frequency range of 4.23–14 GHz. In [20], a wearable textile antenna with a full ground plane was designed for breast cancer detection. Photonic bandgap (PBG) and substrate-integrated waveguide (SIW) technology were utilized for antenna design. The antenna was fed using a grounded CPW (GCPW) through a SIW transition. The results demonstrate that the antenna offered an impedance bandwidth of 21 GHz from 7 GHz to 28 GHz. The presented antenna operates at higher frequencies that are not useful for biomedical applications. In addition, the use of PBG and SIW technologies offers complexities in the fabrication process.

In this article, a CPW-fed pentagonal fractal antenna is designed for near-field microwave imaging applications, especially for breast cancer detection. The results demonstrate that the antenna ranges from 3 GHz to 12.7 GHz, with a peak gain of 3.6 dBi at 8.5 GHz. Furthermore, from the time domain analysis, it is noted that a group delay for both face-to-face and side-by-side configurations is $\leq$1.5 ns, ensuring minimum pulse distortion, which is a fundamental criterion of near-field microwave imaging systems. To further demonstrate the suitability of the proposed antenna, a comparison is presented among proposed and previously published UWB antennas meant for microwave imaging applications (see Table 1).

From Table 1, it can be noted that all the antennas have fractional bandwidth >100%. The designs presented in [9,10,20] have maximum and approximately equal fractional bandwidth, but their electrical dimensions are large in comparison to the proposed design. The rest of the antennas exhibit low fractional bandwidth compared to the proposed antenna design. Furthermore, the proposed fractal antenna offers a high impedance bandwidth compared to the designs presented in [6–8,10,12,17,18].

Table 1. Comparative analysis among proposed and previously presented planar monopole antennas for microwave imaging applications.

Ref.	Dimensions		Dielectric Material	Dielectric Constant	Frequency Band (GHz)	Fractional Bandwidth (%)	Impedance Bandwidth (GHz)	Peak Gain (dBi)	Average Efficiency (%)
	(mm^2)	(λ^2)							
[6]	20 × 25	0.47 × 0.59	FR-4	4.3	3.19–11.03	110.26	7.84	6	80
[7]	33.14 × 14.90	0.77 × 0.34	FR-4	4.4	3–11	114.28	8	4.74	–
[8]	31 × 31	0.72 × 0.72	Rogers RT/Duroid 5870	2.33	3.04–11	113.39	7.96	5	–
[9]	29 × 27	0.87 × 0.81	FR-4	4.4	3–15	133.33	12	–	–
[10]	51 × 95	0.93 × 1.74	FR-4	4.4	1–10	163.63	9	–	–
[12]	23.1 × 32	0.58 × 0.8	FR-4	4.6	3.1–12	117.88	8.9	3.54	–
[17]	20 × 28 16 × 22	0.49 × 0.69 0.39 × 0.54	FR-4	4.4	2.95–12	121	9.05	4 3.7	– –
[18]	16 × 21	0.42 × 0.55	FR-4	4.4	3.4–12.5	114.5	9.1	5	85
[19]	10.2 × 15.5	0.3 × 0.47	FR-4	4.3	4.23–14	107	9.77	5	85
[20]	50 × 60	2.9 × 3.5	Denim substrate	1.4	7–28	120	21	10	88.5
Proposed	24 × 30	0.62 × 0.78	Rogers RT/Duroid 5880	2.2	3–12.7	123.56	9.7	3.6	88

2. Pentagonal Fractal Antenna Design

Figure 2 illustrates the geometry of the proposed UWB antenna. The proposed design is composed of a modified CPW-fed pentagonal fractal radiator, printed on a low-loss Rogers RT/Duroid 5880 dielectric substrate with a relative permittivity (ε_r) of 2.2. The thickness of the dielectric substrate for the antenna design is chosen to be 0.787 mm. The overall dimensions of the antenna are 24 × 30 mm^2. From Figure 2, one can note that a trapezoidal ground plane is used for better impedance matching in the band of interest. Furthermore, the CPW feed technique is utilized because it is easy to design and fabricate and it provides low losses [21]. The rest of the design parameters' values are as follows: W_S = 24 mm, L_S = 30 mm, W_f = 2.5 mm, L_f = 12 mm, t = 1.5 mm, g = 0.3 mm, L_g = 5.5 mm, W_g = 4.2 mm, R_b = 3 mm, R_e = 1 mm, S_1 = 9.6 mm, S_2 = 7.6 mm, S_3 = 5.4 mm, S_4 = 3 mm, R_1 = 7 mm, R_2 = 5 mm, and R_3 = 2.8 mm.

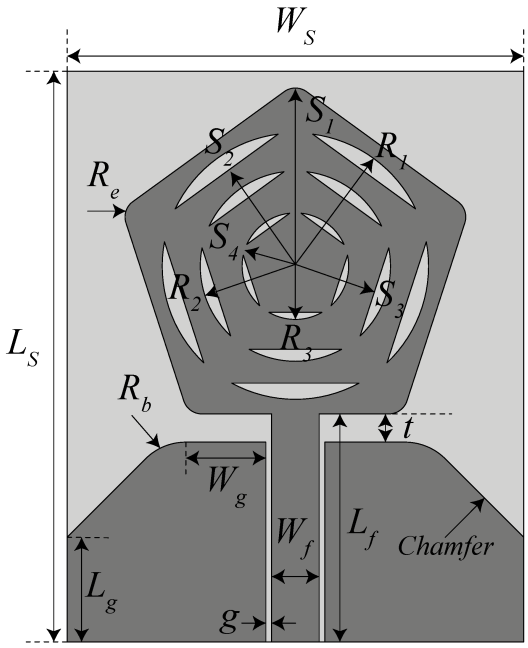

Figure 2. Geometry of the proposed CPW-fed pentagonal fractal antenna.

The design steps of the proposed CPW-fed pentagonal fractal antenna are shown in Figure 3a–d. In the first step, a CPW-fed circle-inscribed pentagonal radiator is designed,

as shown in Figure 3a. The pentagonal radiator's dimensions are calculated using the following expression [22].

$$f_l = \frac{7.2}{(L + r + p) \times k} \quad \text{GHz} \tag{1}$$

where

$$L = 2A, \quad r = \frac{A}{4} \tag{2}$$

where A denotes the radius of the of the pentagonal radiator, which is equal to 9.6 mm. The parameters f_l and k in Equation (1) correspond to the lowest operating frequency of the antenna and the effective relative permittivity (ε_{reff}) of the dielectric substrate, respectively.

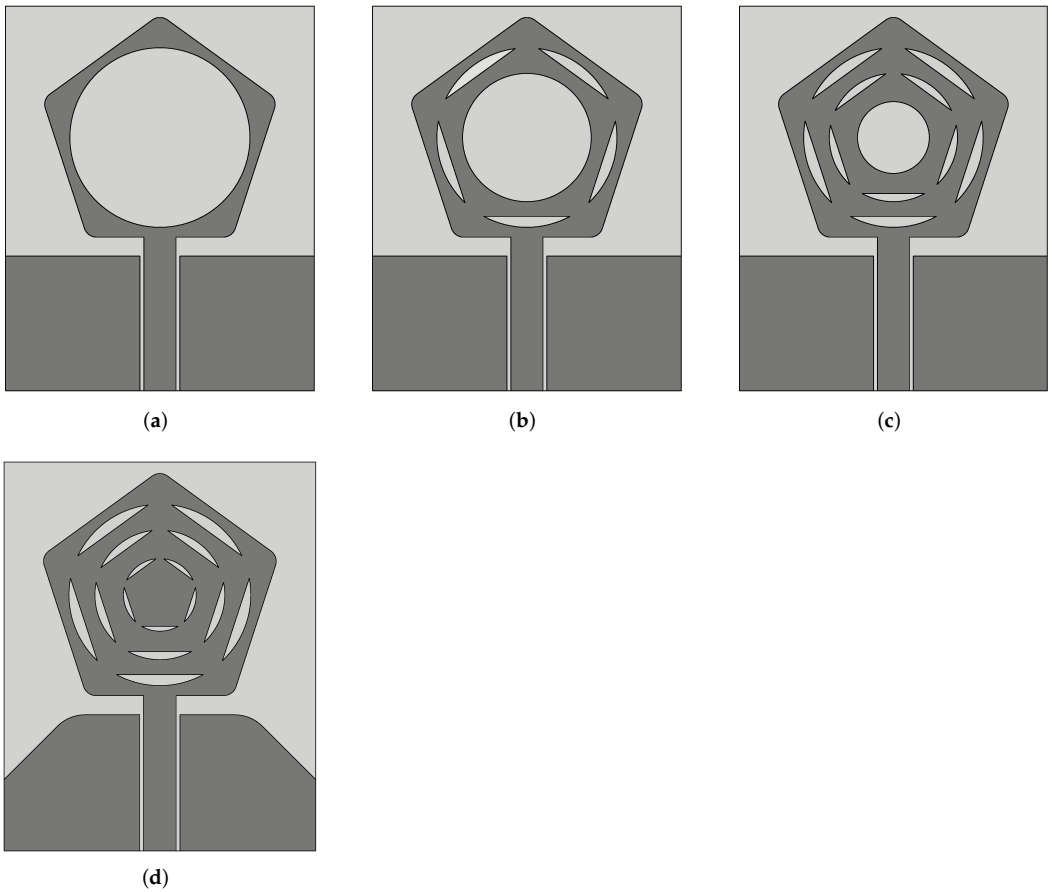

Figure 3. Design evolution of the proposed CPW-fed pentagonal fractal antenna (**a**) Step 1, (**b**) Step 2, (**c**) Step 3, and (**d**) Step 4 (proposed).

The antenna design shown in Figure 3a is simulated in the CST Microwave Studio and the respective reflection coefficient (S_{11}) is given in Figure 4. From the figure, it is observed that the design shown in Figure 3a provides a dual-band response at 4 GHz and around 12 GHz. In the second step, another circle-inscribed pentagonal patch is added in the Step-1 design, as shown in Figure 3b. This modification tends to excite higher order modes and ultimately leads to a UWB response in the band of interest (see Figure 4, Step-2). For improved matching, another pentagonal radiator is added in the Step-2 design, as depicted in Figure 3c. This design offers improved impedance matching in the band of interest, as shown in Figure 4. To further optimize the response, another pentagonal patch is designed with the Step-3 design, as shown in Figure 3d. In this step, the ground plane shape is changed to a trapezoidal shape (see Figure 3d). This modification led to a UWB response in the frequency range of 3.38–12.89 GHz, as shown in Figure 4.

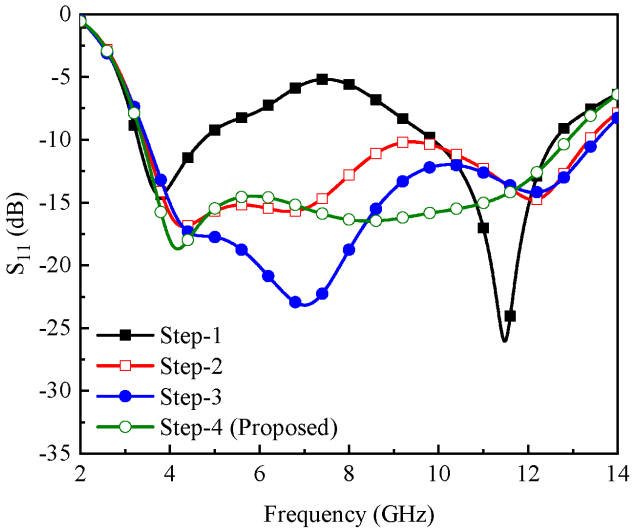

Figure 4. Reflection coefficient (S_{11}) of different antenna designs shown in Figure 3.

The simulated surface current distribution plots for the proposed antenna are shown in Figure 5. The surface current is plotted for three different frequencies, i.e., 4 GHz, 8 GHz, and 12 GHz. It is evident from the figure that at 4 GHz, the dense current is distributed on the feed line, on the edges of the ground plane, and in the lower portion of the patch radiator, as shown in Figure 5a. For higher frequencies, the current is uniformly distributed on the surface of the radiator and modified the CPW ground plane (see Figure 5b,c).

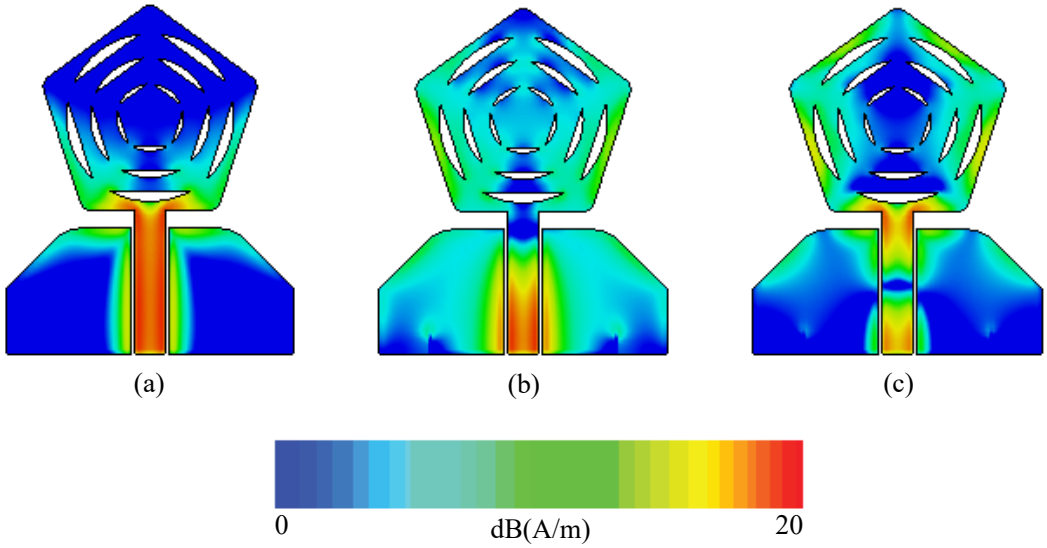

Figure 5. Simulated surface current distribution of the proposed CPW-fed pentagonal fractal antenna at (**a**) 4 GHz, (**b**) 8 GHz, and (**c**) 12 GHz.

A parametric study was performed to understand the behavior of the proposed UWB antenna by varying the gap between the microstrip feeding line and the ground plane, denoted as g, and the gap between the ground plane and the main radiator, denoted as t. From Figure 6a, it is observed that when the value of g is increased from 0.3 mm to 0.9 mm, the bandwidth of the antenna decreases. The maximum impedance matching is obtained for g = 0.3 mm (see Figure 6a). On the other hand, when the value of t is changed from 0.5 mm to 1.5 mm, the impedance bandwidth of the antenna improves, as shown in Figure 6b. For t >1.5 mm, the bandwidth of the antenna is reduced (see Figure 6b).

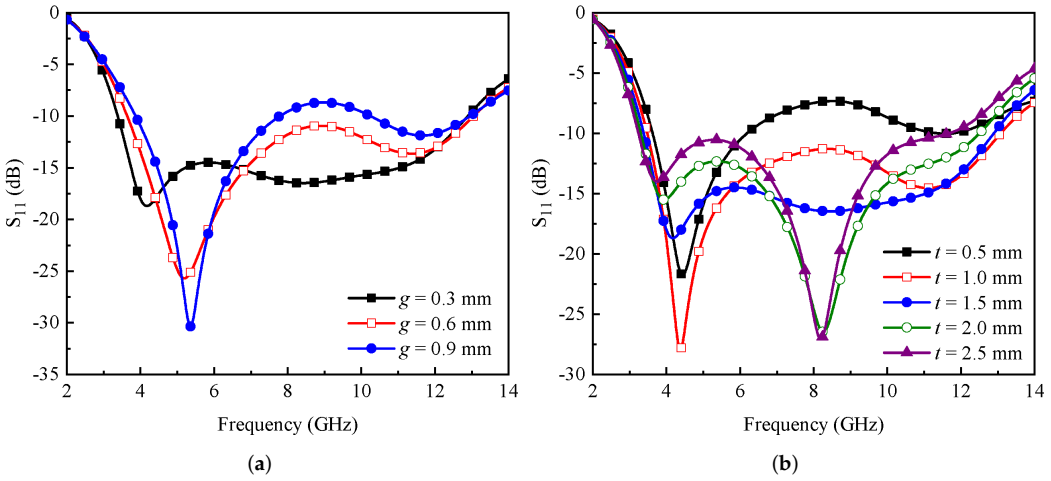

Figure 6. Effect of parameter (**a**) g and (**b**) t on the antenna's performance.

3. Fabricated Prototype and Measurements

To verify the simulation results, the designed antenna was fabricated using the miling process. The prototype of the fabricated antenna is shown in Figure 7a. The S_{11} of the proposed antenna was measured by Rohde Schwarz (R&S) using the vector network analyzer (VNA) ZVA-67. The simulated and measured S_{11} characteristics are shown in Figure 7b. The antenna has a computed impedance bandwidth of 9.51 GHz in the frequency range of 3.38–12.89 GHz and a measured impedance bandwidth of 9.7 GHz in the frequency range of 3–12.7 GHz (see Figure 7b). Some discrepancies are observed between the simulated and measured results, which could arise due to fabrication tolerances, SMA connector losses, and the scattering measurement environment.

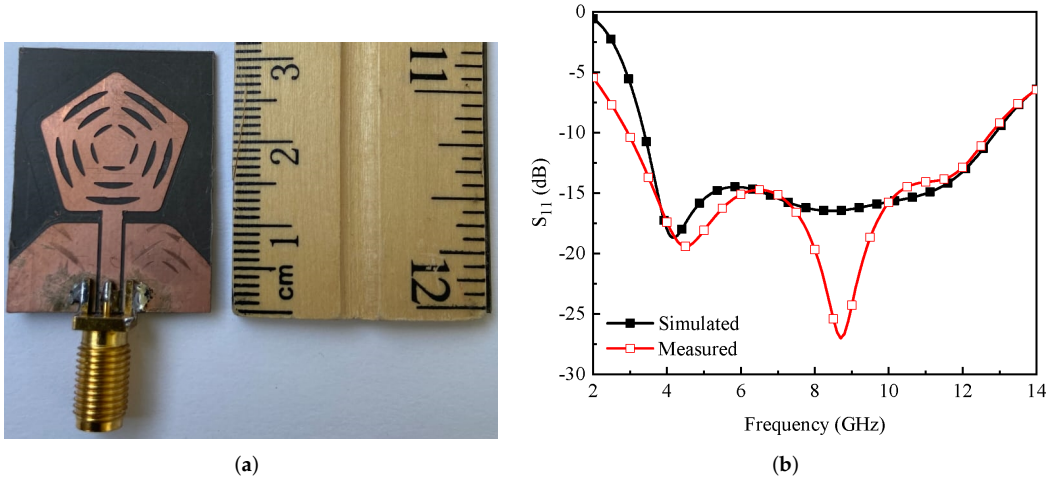

Figure 7. (**a**) Fabricated prototype. (**b**) Simulated and measured S_{11} of the proposed CPW-fed pentagonal fractal antenna.

The simulated and measured radiation characteristics of the proposed fractal antenna are shown in Figure 8. For both the YZ and XZ planes, radiation characteristics are observed at three different frequencies: 4 GHz, 8 GHz, and 12 GHz. From the figure, it is observed that the designed antenna exhibits bi-directional radiation properties for the YZ plane and omnidirectional characteristics for the XZ-plane. It is also observed from Figure 8 that the radiation patterns are almost constant for the entire operating bandwidth, which is a useful property for microwave imaging applications.

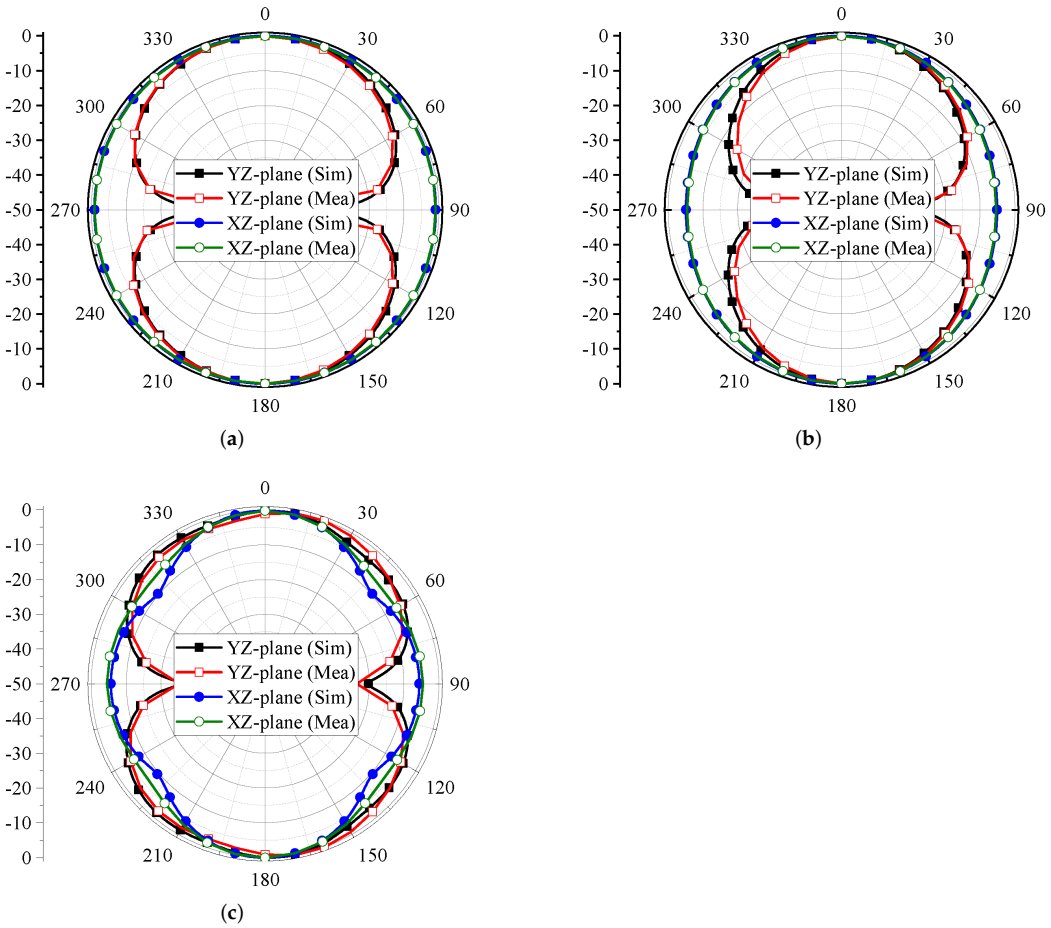

Figure 8. Simulated and measured radiation characteristics of the proposed CPW-fed pentagonal fractal antenna at (**a**) 4 GHz, (**b**) 8 GHz, and (**c**) 12 GHz.

Figure 9 shows the realized gain and efficiency of the proposed antenna. The peak gain of the antenna is noted to be 3.6 dBi at 8.5 GHz, while the minimum gain is 0.6 dBi at 3 GHz, as shown in Figure 9. Furthermore, the efficiency of the antenna is noted to be >80% for the entire operating bandwidth (see Figure 9).

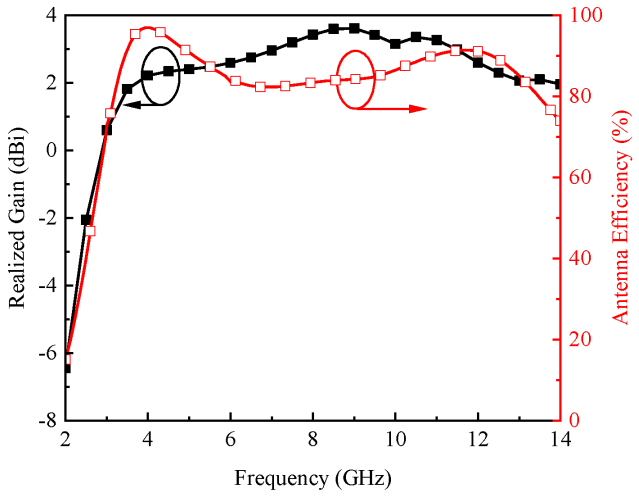

Figure 9. Realized gain and efficiency of the proposed CPW-fed pentagonal fractal antenna.

4. Time Domain Analysis

For near-field microwave imaging applications, it is necessary to assess the performance of the antenna in the time domain [23]. For this purpose, two identical antennas are placed 30 cm apart from each other in two different configurations, i.e., face to face and side by side, respectively, as shown in Figure 10a,b, in which both the antennas work in the transceiver mode.

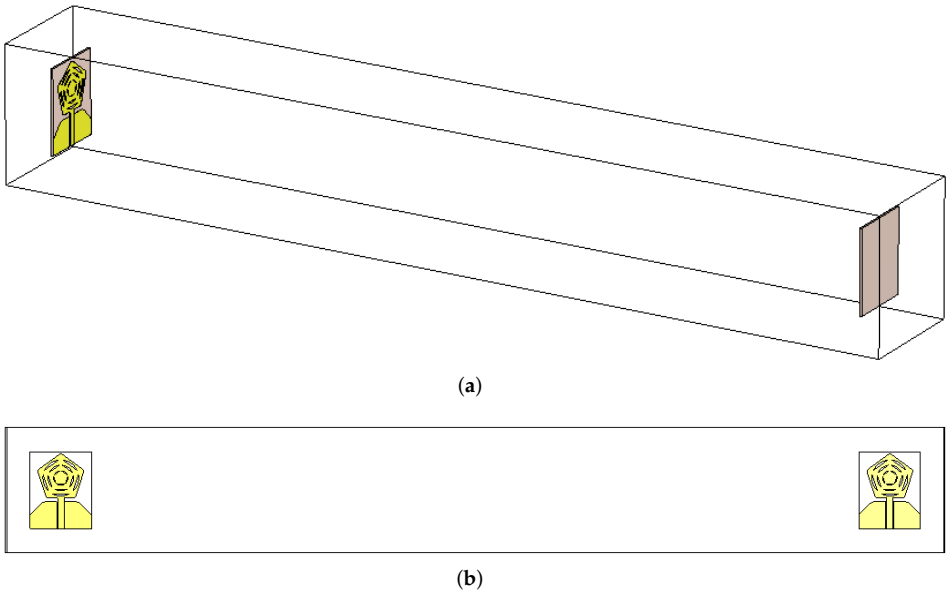

(**a**)

(**b**)

Figure 10. (**a**) Face-to-face and (**b**) side-by-side configuration for the evaluation of time domain performance of the proposed antenna CPW-fed pentagonal fractal antenna.

To excite the antennas, a Gaussian pulse, centered at 8 GHz with a frequency band of 1–15 GHz, is utilized. Figure 11a shows the normalized amplitudes of both input and output signals for both configurations. The cross-correlation between transmitted and received signals is calculated using Equation (3), which is known as the fidelity factor (FF) [24].

$$FF = \max\left[\frac{\int_{-\infty}^{\infty} Y_t(t)Y_r(t+\tau)d\tau}{\int_{-\infty}^{\infty}|Y_t(t)|^2dt\int_{-\infty}^{\infty}|Y_r(t)|^2dt}\right] \quad (3)$$

where $Y_t(t)$ and $Y_r(t)$ represent transmitted and received signals, respectively; and τ represents the group delay. The FF values for face-to-face and side-by-side configurations are noted to be 96.85% and 88.52%, respectively. The high value of FF for the face-to-face configuration shows that the transmitted signal will be less distorted.

The group delay for both the configurations, shown in Figure 10, is presented in Figure 11b. The group delay is defined as *the negative rate of change of the transfer function phase, $\phi(\omega)$ with respect to frequency*. The group delay quantifies the transition time taken by the signal to travel through a device [23]. Mathematically, it can be calculated as:

$$\tau(\omega) = -\frac{d\phi(\omega)}{d\omega} = -\frac{d\phi(\omega)}{2\pi df} \quad (4)$$

For UWB applications, $|\tau| \leq 2$ ns is desirable to ensure linearity of the phase in the far-field region. From Figure 11b, one can observe that the $|\tau|$ value is ≤ 1.5 ns for the entire frequency range [25].

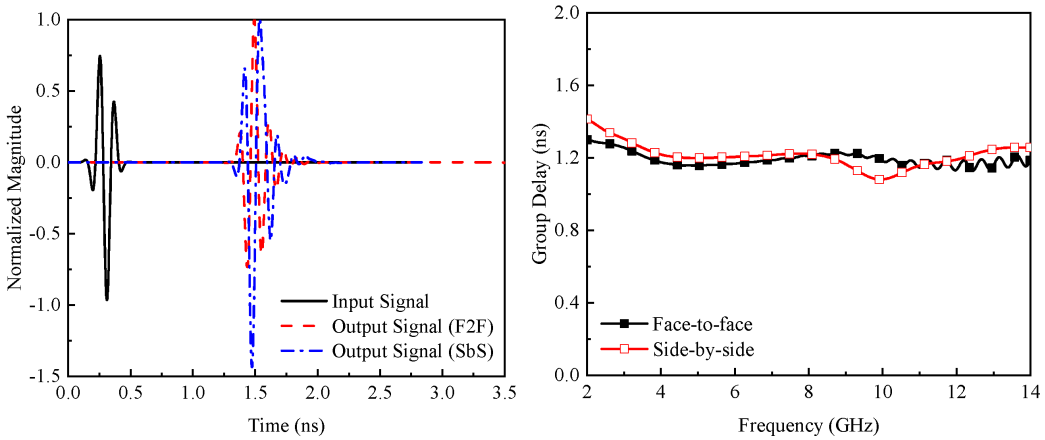

Figure 11. (**a**) Pulse response and (**b**) group delay of the proposed antenna CPW-fed pentagonal fractal antenna.

5. Conclusions

A compact UWB planar antenna is reported for near-field microwave imaging applications. The radiator geometry consists of a modified CPW-fed pentagonal fractal structure. To improve the impedance matching, a trapezoidal-shaped ground plane is utilized. The proposed design has an impedance bandwidth of 9.7 GHz, ranging from 3 GHz to 12.7 GHz, and offers a fractional bandwidth of 123.56%. It is also observed from the results that the proposed antenna exhibits constant radiation characteristics in the operating bandwidth, which is useful for near-field microwave imaging. The performance of the proposed antenna is also assessed in the time domain, and acceptable characteristics are observed.

Author Contributions: Conceptualization, M.A.K., U.R. and S.H.K.; methodology, M.A.K., A.N.N. and S.H.K.; software, U.R., H.Ş.S., U.R., S.H.K. and S.M.A.; validation, M.A.K., U.R., S.H.K. and S.M.A.; formal analysis, H.Ş.S. and A.N.N.; investigation, U.R., A.N.N. and S.H.K.; resources, H.Ş.S., A.N.N. and S.M.A.; writing—original draft preparation, M.A.K. and S.H.K.; writing—review and editing, U.R., H.Ş.S., A.N.N. and S.M.A.; visualization, U.R.; supervision, A.N.N. and S.H.K.; project administration, M.A.K., U.R. and A.N.N.; funding acquisition, S.M.A. All authors have read and agreed to the published version of the manuscript.

Funding: This research received no external funding.

Conflicts of Interest: The authors declare no conflict of interest.

References

1. Fear, E.C.; Hagness, S.C.; Meaney, P.M.; Okoniewski, M.; Stuchly, M.A. Enhancing breast tumor detection with near-field imaging. *IEEE Microw. Mag.* **2002**, *3*, 48–56. [CrossRef]
2. Fear, E.; Stuchly, M. Microwave detection of breast cancer. *IEEE Trans. Microw. Theory Tech.* **2000**, *48*, 1854–1863.
3. Wells, P.N. Ultrasound imaging. *Phys. Med. Biol.* **2006**, *51*, R83. [CrossRef] [PubMed]
4. Nass, S.J.; Henderson, I.C.; Lashof, J.C. *Mammography and Beyond: Developing Technologies for the Early Detection of Breast Cancer*; National Academy Press: Washington, DC, USA, 2001.
5. El Misilmani, H.M.; Naous, T.; Al Khatib, S.K.; Kabalan, K.Y. A survey on antenna designs for breast cancer detection using microwave imaging. *IEEE Access* **2020**, *8*, 102570–102594. [CrossRef]
6. Ojaroudi, M.; Civi, Ö.A. High efficiency loop sleeve monopole antenna for array based UWB microwave imaging systems. In Proceedings of the 2016 IEEE International Symposium on Antennas and Propagation (APSURSI), Fajardo, PR, USA, 26 June–1 July 2016; pp. 1781–1782.
7. Danjuma, I.M.; Akinsolu, M.O.; See, C.H.; Abd-Alhameed, R.A.; Liu, B. Design and optimization of a slotted monopole antenna for ultra-wide band body centric imaging applications. *IEEE J. Electromagn. Microw. Med. Biol.* **2020**, *4*, 140–147. [CrossRef]
8. Mahmud, M.; Islam, M.T.; Samsuzzaman, M. A high performance UWB antenna design for microwave imaging system. *Microw. Opt. Technol. Lett.* **2016**, *58*, 1824–1831. [CrossRef]

9. Subramanian, S.; Sundarambal, B.; Nirmal, D. Investigation on simulation-based specific absorption rate in ultra-wideband antenna for breast cancer detection. *IEEE Sens. J.* **2018**, *18*, 10002–10009. [CrossRef]
10. Lee, D.; Nowinski, D.; Augustine, R. A UWB sensor based on resistively-loaded dipole antenna for skull healing on cranial surgery phantom models. *Microw. Opt. Technol. Lett.* **2018**, *60*, 897–905. [CrossRef]
11. Wu, T.; King, R. The cylindrical antenna with nonreflecting resistive loading. *IEEE Trans. Antennas Propag.* **1965**, *13*, 369–373. [CrossRef]
12. Islam, M.; Islam, M.; Samsuzzaman, M.; Faruque, M.; Misran, N. Microstrip line-fed fractal antenna with a high fidelity factor for UWB imaging applications. *Microw. Opt. Technol. Lett.* **2015**, *57*, 2580–2585. [CrossRef]
13. Ahadi, M.; Isa, M.B.M.; Saripan, M.I.B.; Hasan, W.Z.W. Square monopole antenna for microwave imaging, design and characterisation. *IET Microw. Antennas Propag.* **2014**, *9*, 49–57. [CrossRef]
14. Halili, K.; Ojaroudi, M.; Ojaroudi, N. Ultrawideband monopole antenna for use in a circular cylindrical microwave imaging system. *Microw. Opt. Technol. Lett.* **2012**, *54*, 2202–2205. [CrossRef]
15. Ojaroudi, N.; Ghadimi, N. Omnidirectional microstrip monopole antenna design for use in microwave imaging systems. *Microw. Opt. Technol. Lett.* **2015**, *57*, 395–401. [CrossRef]
16. Abdollahvand, A.; Pirhadi, A.; Ebrahimian, H.; Abdollahvand, M. A compact UWB printed antenna with bandwidth enhancement for in-body microwave imaging applications. *Prog. Electromagn. Res.* **2014**, *55*, 149–157. [CrossRef]
17. Lasemi, Z.; Atlasbaf, Z. Impact of Fidelity Factor on Breast Cancer Detection. *IEEE Antennas Wirel. Propag. Lett.* **2020**, *19*, 1649–1653. [CrossRef]
18. Islam, M.; Islam, M.; Samsuzzaman, M.; Faruque, M. A negative index metamaterial antenna for UWB microwave imaging applications. *Microw. Opt. Technol. Lett.* **2015**, *57*, 1352–1361. [CrossRef]
19. Afifi, A.; Abdel-Rahman, A.B.; Allam, A.; Abd El-Hameed, A.S. A compact ultra-wideband monopole antenna for breast cancer detection. In Proceedings of the 2016 IEEE 59th International Midwest Symposium on Circuits and Systems (MWSCAS), Abu Dhabi, United Arab Emirates, 16–19 October 2016; pp. 1–4.
20. Mahmood, S.N.; Ishak, A.J.; Saeidi, T.; Soh, A.C.; Jalal, A.; Imran, M.A.; Abbasi, Q.H. Full Ground Ultra-Wideband Wearable Textile Antenna for Breast Cancer and Wireless Body Area Network Applications. *Micromachines* **2021**, *12*, 322. [CrossRef]
21. Rafique, U.; ud Din, S.; Khalil, H. Compact CPW-fed super wideband planar elliptical antenna. *Int. J. Microw. Wirel. Technol.* **2021**, *13*, 407–414. [CrossRef]
22. Ray, K.P. Design aspects of printed monopole antennas for ultra-wide band applications. *Int. J. Antennas Propag.* **2008**, *2008*. [CrossRef]
23. Wiesbeck, W.; Adamiuk, G.; Sturm, C. Basic properties and design principles of UWB antennas. *Proc. IEEE* **2009**, *97*, 372–385. [CrossRef]
24. Singhal, S.; Singh, A.K. CPW-fed hexagonal Sierpinski super wideband fractal antenna. *IET Microw. Antennas Propag.* **2016**, *10*, 1701–1707. [CrossRef]
25. Kwon, D.H. Effect of antenna gain and group delay variations on pulse-preserving capabilities of ultrawideband antennas. *IEEE Trans. Antennas Propag.* **2006**, *54*, 2208–2215. [CrossRef]